Proteolytic Processing Converts the Repelling Signal Sema3E into an Inducer of Invasive Growth and Lung Metastasis

Claus Christensen,[1] Noona Ambartsumian,[1] Giorgio Gilestro,[3] Birthe Thomsen,[2] Paolo Comoglio,[3] Luca Tamagnone,[3] Per Guldberg,[1] and Eugene Lukanidin[1]

[1]Institute of Cancer Biology, [2]Department of Biostatistics and Electronic Data Processing, Institute of Cancer Epidemiology, Danish Cancer Society, Copenhagen, Denmark; and [3]Institute of Cancer Research and Treatment, University of Turin, Candiolo, Italy

Abstract

We have previously shown that the expression of a semaphorin, known as a repelling cue in axon guidance, Sema3E, correlates with the ability to form lung metastasis in murine adenocarcinoma cell models. Now, besides providing evidence for the relevance of SEMA3E to human disease by showing that SEMA3E is frequently expressed in human cancer cell lines and solid tumors from breast cancer patients, we show biological activities of Sema3E, which support the implication of Sema3E in tumor progression and metastasis. *In vivo*, expression of Sema3E in mammary adenocarcinoma cells induces the ability to form experimental lung metastasis, and *in vitro*, the Sema3E protein exhibits both migration and growth promoting activity on endothelial cells and pheochromocytoma cells. This represents the first evidence of a metastasis-promoting function of a class 3 semaphorin, as this class of genes has hitherto been implicated in tumor biology only as tumor suppressors and negative regulators of growth. Moreover, we show that the full-size Sema3E protein is converted into a p61-Sema3E isoform due to furin-dependent processing, and by analyzing processing-deficient and truncated forms, we show that the generation of p61-Sema3E is required and sufficient for the function of Sema3E in lung metastasis, cell migration, invasive growth, and extracellular signal–regulated kinase 1/2 activation of endothelial cells. These findings suggest that certain breast cancer cells may increase their lung-colonizing ability by converting the growth repellent, Sema3E, into a growth attractant and point to a type of semaphorin signaling different from the conventional signaling induced by full-size dimeric class 3 semaphorins. (Cancer Res 2005; 65(14): 6167-77)

Introduction

Metastasis is a multistep process in which cancer cells invade the surrounding tissue at the primary tumor site, enter the vascular system, and finally extravasate and grow in other organs. Although cancer cells in circulation may efficiently arrest in the first capillary bed they encounter, the metastases only develop in organs where the cancer cells and the microenvironment are compatible (1–4). Consequently, many genes that control metastatic growth encode secretory or cell surface proteins, which mediate intercellular communication between tumor cells and cells of the target organ (5–7). In addition, different sets of genes may determine metastasis to different organs (8).

In an attempt to identify genes involved in lung metastasis of breast cancer cells, we have previously compared gene expression profiles of metastatic and nonmetastatic subpopulations derived from murine mammary adenocarcinomas. We identified *semaphorin 3E* (*Sema3E*/previously *M-semaH*; ref. 9) as a gene expressed in all cell lines that are capable of metastasizing to lungs but only in a few nonmetastatic cell lines (10). Semaphorins belong to a diverse group of genes that encode growth guidance cues (the others include the ephrin, netrin, and slit genes). These cues cooperate with growth factors to achieve the proper development of the nervous and cardiovascular systems (11–13). Presumably reflecting their natural role in cardiovascular development, growth guidance cues and their receptors have been implicated in tumor angiogenesis (14, 15). Hence, SEMA4D has been shown to be an angiogenic factor as well as a stimulator of invasive growth (16, 17), whereas SEMA3A and SEMA3F act as antagonists of vascular endothelial growth factor signaling through binding to neuropilin coreceptors (18, 19). Notably, the *SEMA3B* and *SEMA3F* genes are located in chromosomal region 3p21.3 that is frequently deleted in lung cancer (20), and in accordance with a tumor-suppressive role, ectopic expression of SEMA3B and SEMA3F leads to apoptosis and reduced growth in xenografted human tumors (21, 22). In addition, SEMA3F acts as a direct chemorepellent for endothelial cells and when overexpressed in melanoma cells, SEMA3F induces a poorly vascularized, nonmetastatic tumor type (23).

To date, no semaphorin has been shown to promote metastasis. The strongest candidate for this role, Sema3E, belongs to the same class of secreted semaphorins as the tumor-suppressive semaphorins, SEMA3B and SEMA3F (i.e., class 3), and it is unclear how these structurally related semaphorins could fulfil opposing roles during tumor progression. Previously, growth-repelling activities have been associated with dimeric forms of full-size class 3 semaphorins (24, 25), and furin-dependent processing has been shown to down-regulate these activities (26). Here, we show that Sema3E promotes lung metastasis *in vivo* and confirm that Sema3E possesses growth and motility stimulating activity *in vitro*. We find that both these activities are associated with a p61-Sema3E isoform, which is generated from full-size Sema3E proteins by the same furin-dependent processing known to down-regulate the repellent activity.

Materials and Methods

Cell lines and tumor tissues. Tumor tissues were obtained from Rigshospitalet (Copenhagen, Denmark). SVEC4-10 cells were obtained from

Note: Supplementary data for this article are available at Cancer Research Online (http://cancerres.aacrjournals.org/).

Correspondence: Claus Christensen, Institute of Cancer Biology, Danish Cancer Society, Strandboulevarden 49, DK-2100 Copenhagen, Denmark. Phone: 45-3525-7387; E-mail: clc@cancer.dk.

the American Type Culture Collection (Manassas, VA). The PC12-E2 cell line was obtained from Dr. Elisabeth Bock (Panum Institute, Copenhagen, Denmark). Lung microcapillary endothelial cells and hepatic sinusoidal endothelial cells (HSE) cultures were provided by Dr. Jun-Ichi Hamada (Division of Cancer-Related Genes Institute for Genetic Medicine, Hokkaido University, Sapporo, Japan) and grown as described (27). The 168FARN cells were grown as previously described (10).

Reverse transcription-PCR analysis of SEMA3E mRNA. Total RNA was isolated from cell lines and tumor tissues using the NucleoSpin Kit (Macherey-Nagel, Düren, Germany) and reverse transcribed using random hexamers and Superscript III (Invitrogen, Carlsbad, CA). The PCR was done in a block thermocycler or the LightCycler (Roche, Indianapolis, IN) using primers 5′-GATACGGAACCACCAAGGAC-3′ and 5′-CTTCTTCCATTGATTCCATTTC-3′ for SEMA3E, 5′-TCCAAGCGGAGCCATGTCTG-3′ and 5′-AGAATCTTGTCCCCTGTGGTGGA-3′ for PBGD, and 5′-AGGGGGGAGCCAAAAGGG-3′ and 5′-GAGGAGTGGGTGTCGCTGTTG-3′ for glyceraldehyde-3-phosphate dehydrogenase.

Sema3E expression constructs. The entire open reading frame of Sema3E was amplified by PCR and cloned onto pcDNA3.1(−)/zeo^R and pcDNA3.1-myc-his/neo^R using *Apa*I linkers. A pcDNA3.1-mychis/neo^R vector encoding Sema3E (+)(−)myc was obtained from Dr. Alain Chedotal (Hôpital de la Salpêtrière, Paris). The sequence encoding KRRFRR was changed into KRSFGG by PCR site directed mutagenesis using the primers 5′-TTCGGCGGGCAGGACGTTCGGCATGGCAACGCC-3′ and 5′-GCTTCTCTTTGCGTGTGCACCTGTTGGGTAGTA-3′. This way vectors encoding Sema3E(−)(+)myc and Sema3E(−)(−)myc were obtained from pcDNA3.1(−)/zeo^R: sema3E(+)(+)myc and pcDNA3.1/neo^R: sema3E(+)(−)myc, respectively. A pcDNA3.1/zeo^R construct encoding truncated Sema3E-myc (p61-Sema3E^{TR}-myc) was generated from a previously made pSecTag:AP-myc vector encoding alkaline phosphatase fused to amino acids 32 to 560 of Sema3E. This vector was cut with *Xho*I and *Pme*I, and the released fragment ligated onto *Xho*I and *Eco*RV digested pcDNA3.1/zeo^R/sema3E.

Transfections. 168FARN cells were transfected by electroporation followed by selection using 500 μg/mL zeocin (Invitrogen). COS-7 cells were transfected by the LipofectAMINE 2000 (Invitrogen) or DEAE-dextran method. HEK-293 cells were transfected by the LipofectAMINE 2000 method.

Experimental lung metastasis. Cells (10^5) in 200 μL PBS were injected i.v. in the tail vein of female BALB/c mice (age 10-12 weeks). All transfected cells were injected before passage 11 posttransfection. Mice were sacrificed between days 20 and 35, and total lung weight was measured. Statistical analysis was done using a linear mixed model that assumes exponential growth of lung weights with a systematic effect of the type of transfection [no transfection, vector, wild-type Sema3E, p61-Sema3E^{TR}-myc, or Sema3E(−)(+)myc].

Fractionation of conditioned medium. Cells were grown to 70% confluency, washed twice and incubated with a volume of serum-free DMEM/F12 medium resulting in 5×10^5 adherent cells/mL. After 24, 48, or 72 hours, conditioned medium was collected, filtrated, and then either concentrated 50× or 100× for use in immunoblot analysis with 1.1 μg/mL of affinity-purified anti-Sema3E polyclonal antibodies or stored at −80°C with 0.1% bovine serum albumin (BSA) and 25 mmol/L HEPES (pH 7.4). The separation of Sema3E isoforms was done from 400 mL of conditioned medium collected after 72 hours from Sema3E-transfected COS-7. The medium was adjusted to 50 mmol/L NaCl, 10 mmol/L Tris (pH 7) and passed through heparin Sepharose (Pierce, Rockford, IL). Proteins were eluted with a NaCl gradient, and fractions containing Sema3E were pooled, dialyzed, and concentrated to 1 mL. The concentrate was loaded onto a XK16 column containing Superdex 200 (Amersham Biosciences, Piscataway, NJ) and separated into 3-mL fractions at 0.5 mL/min. Samples were removed for immunoblot analysis and quantification of protein and stored for assays of activity.

Recombinant p61-Sema3E^{TR}-mychis. The sequence encoding amino acids 32 to 560 of Sema3E was PCR amplified and ligated onto pPICZαB:myc-his/zeo^R (Invitrogen) using *Pst*I and *Xba*I sites. The resulting vector encoded truncated Sema3E-mychis (p61-Sema3E^{TR}-mychis). *Pichia pastoris* strain GS115 was transformed by electroporation. Zeocin-resistant clones were induced for Sema3E expression by growing in potassium phosphate–buffered minimal medium (pH 6) containing Histidine and 0.5% (v/v) methanol. The p61-Sema3E^{TR}-mychis protein was purified using Ni^{2+} affinity chromatography.

Polyclonal Sema3E antibody. The sequence encoding amino acids 28 to 98 of Sema3E was ligated onto the pQE30 vector (Qiagen, Valencia, CA) for production of a Histidine-tagged Sema3E peptide in XL1 bacteria and purification using Ni^{2+} affinity chromatography. Polyclonal antibodies were raised in rabbits and affinity purified from the serum using Sepharose beads coupled to the His-Sema3E fragment by CNBr activation. In immunoprecipitations, 100 μg/mL antibody was preincubated with 20 % (v/v) protein A/G Sepharose (Pierce). 5 % (v/v) immunoglobulin-coated beads was added to conditioned medium and mixed for 4 hours at 4°C. The supernatant was tested for remaining biological activity.

Immunohistochemistry. For immunohistochemical staining slides prepared from paraffin-embedded tissues were pretreated with a 25 mg/mL trypsin solution for 20 minutes at 37°C and incubated with 1.1 μg/mL of affinity-purified anti-Sema3E polyclonal antibodies, overnight at 4°C. Sema3E-positive cells were visualized using anti-rabbit biotin conjugated secondary antibodies (DAKO Cytomation, Glostrup, Denmark) together with the TCA-biotin amplification system (Perkin-Elmer, Shelton, CT). Slides were counterstained with Meyers hematoxylin. The specificity was tested by mixing primary antibody with a 5-fold excess of p61-Sema3E^{TR}-mychis protein.

Neurite outgrowth. PC12-E2 cells (5,000) were seeded per cm^2 in poly-L-lysine–coated wells. The next day, the test proteins were given and diluted in a mixture of serum-free DMEM/F12 and conditioned medium from COS-7 cells previously adjusted to produce minimal neurite outgrowth itself. Fractions of conditioned medium were tested using 5 μg total protein/mL. Nerve growth factor (NGF, 200 ng/mL; Roche), basic fibroblast growth factor (200 ng/mL; Sigma, St. Louis, MO) and BSA (Sigma) served as controls. After 48 hours, the cells were fixed with 11% glutaraldehyde for 15 minutes and stained for 15 minutes with 0.1% crystal violet. When using decanoyl-RVKR-chloromethylketone (100 μmol/L, Bachem, Bubendorf, Schwitzerland) the cells were fixed after 24 hours. In each well, 100 to 200 cells were examined to find the percentage of the cells extending neurites longer than twice the cell diameter.

Endothelial cell migration. The migration of SVEC4-10, lung microcapillary endothelial, and HSE cells was tested using blindwell chambers (Receptor Tech., Oxon, United Kingdom). Assays ran for 5 hours. A mixture of fibronectin (4 μg/filter, Sigma) and Perlecan (0.5 ng/filter, Sigma) constituted the substratum, and proteins were tested in DMEM/F12 medium containing 25 mmol/L HEPES (pH 7.4) and 0.1% BSA, or conditioned medium from COS-7. In each experiment, tests were done in triplicate and migrated cells were counted in four random fields per filter. Differences in mean values were analyzed for variance followed by t test.

Proliferation and adhesion assays. Population doubling times were determined by direct cell counting using a nucleometer (Chemometech, Allerød, Denmark). Adhesion to endothelial cells was tested by plating 15,000 SVEC4-10 cells in 96-well plates. The day after, 40,000 168FARN cells were seeded and the assay stopped at 5, 10, 25, and 50 minutes. The experiments were done in sextuplicate and done thrice. Quantification was made as previously described (28).

Invasive growth assays. The endothelial cell invasion assay was done by placing aggregates of SVEC4-10 cells inside extracellular matrix (Biomedical Tech., Stoughton, MA) as previously described (29). Aggregates were grown for 24 hours in conditioned medium collected from transfected HEK-293 cells. The invasive growth of parental and transfected 168FARN cells was tested by growing 10,000 cells inside 0.9 mL of a collagen I mixture in 48-well plates [mixture: 2 mg/mL collagen I (Vitrogen, Leimuiden, the Netherlands), 1× DMEM, 2.4 mg/mL $NaHCO_3$, 20 mM HEPES (pH 7.4), penicillin and streptomycin]. Solidified gel was covered with medium supplemented with 10% fetal bovine serum, either DMEM or conditioned medium from transfected HEK-293 cells. Medium was replaced every third day and after 10-day cultures were evaluated for invasive growth.

Immunoblot analysis of extracellular signal–regulated kinase 1/2. Cells were washed twice with serum-free DMEM/F12 medium and incubated in this medium. The following day, cells were washed again, and 2 hours later, they were incubated in the same kind of medium containing no supplements, 1% serum, hepatocyte growth factor (HGF, 20 ng/mL), or 70 ng/mL p61-Sema3E^{TR}mychis. Lysates were produced using extraction buffer [50 mmol/L Tris-HCl (pH 7.6), 5 mmol/L EDTA, 150 mmol/L NaCl, 10% glycerol, 1% Triton X-100] supplemented with a protease inhibitor cocktail (Sigma-Aldrich, St, Louis, MO). Protein (50 μg) was analyzed by immunoblotting using the PhosphoPlus p44/42 mitogen-activated protein kinase Antibody Kit (Cell Signaling, Beverly, MA).

Results

SEMA3E is expressed in human mammary adenocarcinoma cells. We have previously reported a positive correlation between the expression of Sema3E and the ability of mouse adenocarcinoma cell lines to form lung tumors in the experimental lung metastasis assay (10). To explore the relevance of this finding in humans and thus the grounds for further analysis of Sema3E in cancer, we examined the expression of SEMA3E in human breast cancer cells. Transcripts were detected in 7 of 10 tumor-derived cell lines (70 %). Positive cell lines included MDA-MB-468, MDA-MB-231, MDA-MB-157, MCF-7, ZR75-1, BT-20, and T47D whereas BT549, MDA-MB-453, and the nontransformed mammary epithelial HME1 cells were negative with respect to SEMA3E transcripts (Fig. 1*A*). We also investigated tumor samples obtained from breast cancer patients including node negative (n = 3) and node-positive primary tumors (n = 14). Of the latter, matching pairs of primary tumor and axillary lymph node metastases had been obtained in six cases. Out of a total of 23 samples, primary tumors and metastasis alike, SEMA3E transcripts were detectable in 16 cases (69%; Fig. 1*B*). The number of samples was too limited to allow the investigation of the possible correlation between regional metastasis and SEMA3E expression. However, the frequent existence of SEMA3E transcripts in human breast cancer cell lines and solid tumors, including metastases, clearly showed the relevance of SEMA3E to human disease and thus warranted further investigations into the function of Sema3E in cancer.

Sema3E stimulates experimental lung metastasis. Mouse tumor models are well suited for studies of metastasis as they offer an opportunity for assessment of metastasis *in vivo* using isogenic cell lines and mouse strains. To investigate the possible lung metastasis promoting function of Sema3E, we made use of 168FARN cells, which originate from a mouse mammary adenocarcinoma. These cells do not express endogenous Sema3E and although capable of extravasation, they do not grow in the lungs after i.v. injection in BALB/c mice (10, 30, 31). We first transfected the 168FARN cells with a construct encoding full-length mouse Sema3E and investigated stable clones with polyclonal antibodies raised against the NH_2 terminus of Sema3E. Immunoblot analysis of the conditioned medium from stable clones revealed a band pattern that was specific to Sema3E transfectants (clones SEM-1 and SEM-2) and similar to the pattern in conditioned medium from two metastatic cell lines, CSML-100 and 66cl4, expressing endogenous Sema3E mRNA (10) and COS-7 cells transiently transfected with Sema3E (Fig. 2*A*). This pattern of bands seemed

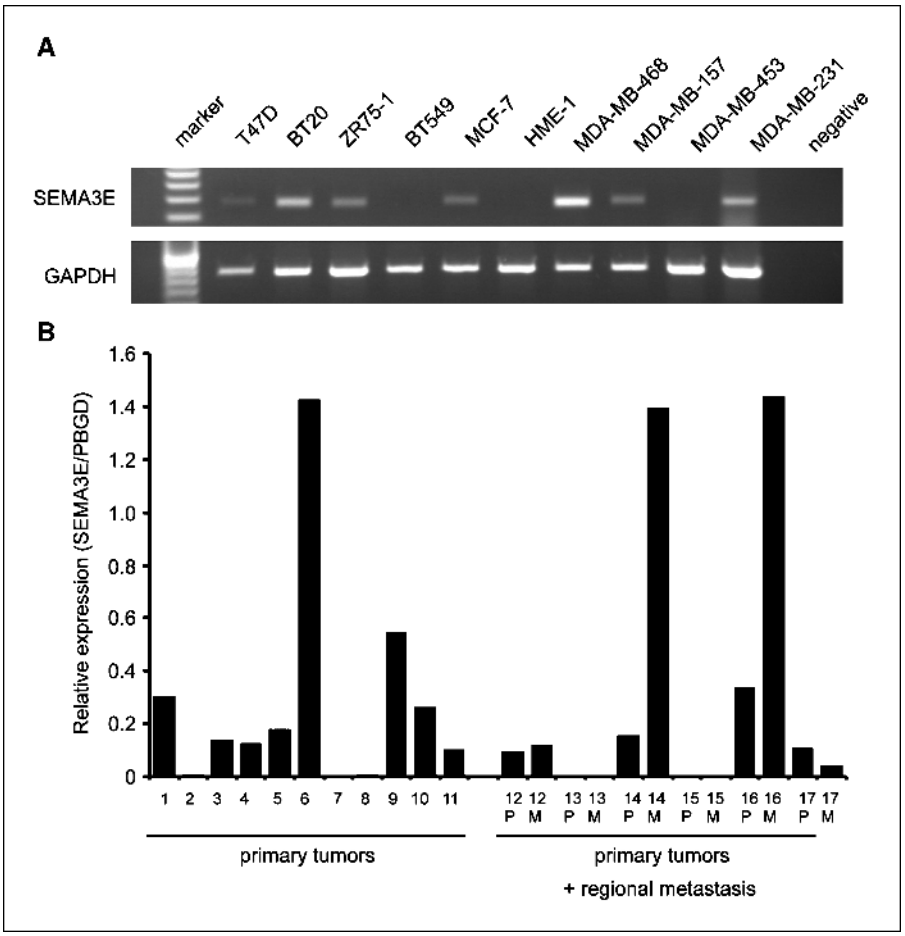

Figure 1. SEMA3E expression in human breast cancer cell lines and breast carcinoma tissues. *A,* SEMA3E mRNA expression in nine breast cancer cell lines and nontransformed mammary HME1 cells was examined by RT-PCR analysis. cDNA was synthesized from 1 μg of total RNA, normalized for PBGD gene messages, and amplified with specific primers to SEMA3E or glyceraldehyde-3-phosphate dehydrogenase (*GAPDH*). The RT-PCR products were separated on a 2% agarose gel and stained with ethidium bromide. *B,* SEMA3E mRNA expression in breast carcinoma tissues was examined by RQ-PCR analysis, relative to PBGD. SEMA3E/PBGD = 1.0 corresponds to the level observed in MDA-MB-468. For six patients, matching pairs of primary tumors (*P*) and axillary lymph node metastases (*M*) were examined.

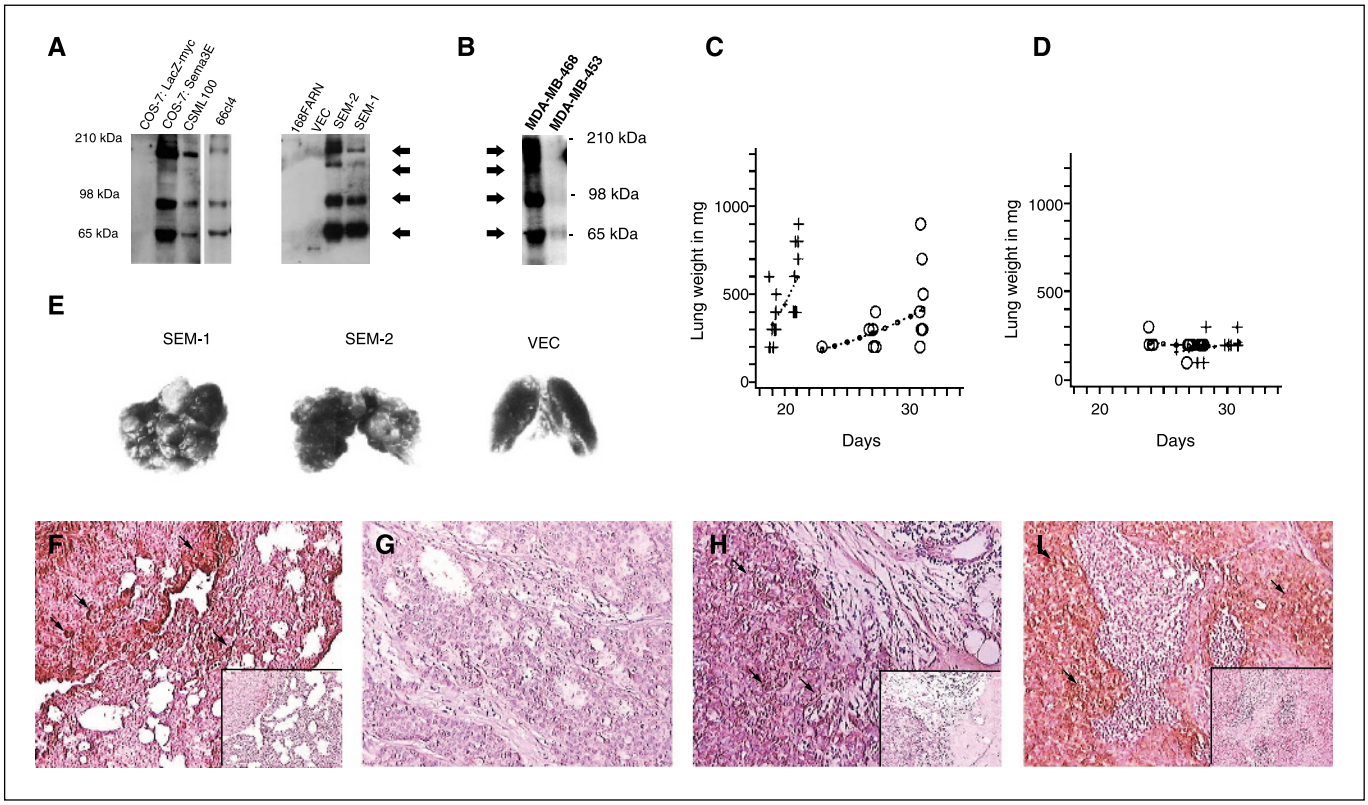

Figure 2. Sema3E promotes experimental lung metastasis. *A,* immunoblot analysis of Sema3E expression in conditioned medium from mouse mammary adenocarcinoma cell lines CSML-100, 66cl-4, and 168FARN, as well as transiently transfected COS-7 cells (LacZ-myc and Sema3E) and stable transfectants of 168FARN cells expressing Sema3E (clones SEM-1 and SEM-2) or no protein (clone *VEC*). The medium was concentrated 50-fold. The detected proteins (*arrows*) have molecular weights of ~174, ~112, ~87, and ~61 kDa, respectively. *B,* immunoblot analysis of Sema3E expression in the conditioned medium from human cancer cell lines MDA-MB-468 and MDA-MB-453. Medium was concentrated 100-fold and analyzed with the polyclonal antibody to mouse Sema3E. Arrows point to the same pattern of bands as observed in the medium from murine cells. *C* and *D,* assessment of tumor growth by measurements of the total lung weights at different time points following i.v. injection. Each point represents one mouse. *C,* mice injected with Sema3E expressing 168FARN cells, clone SEM-1 (+, $n = 18$) and clone SEM-2 (O, $n = 13$). *D,* mice injected with parental 168FARN cells (+; $n = 15$) or mock transfected 168FARN cells, clone VEC (O, $n = 13$). *E,* examples of the macroscopic appearance of the lungs excised from mice injected with Sema3E-expressing 168FARN cells (SEM-1 and SEM-2) or mock-transfected 168FARN cells (*VEC*). *F-I,* immunohistochemical staining of tissues with anti-Sema3E antibody. *F,* mouse lung tissue with metastatic lesion consisting of 168FARN cells expressing Sema3E. *G,* human breast tumor 13 negative for SEMA3E expression. Human breast tumor 16 (*H*) and lymph node metastasis 16 (*I*) expressing SEMA3E. Arrows in (*F-I*) point to Sema3E-positive cells. Controls where staining is blocked by Sema3E protein (*right bottom corner insets*).

to be a conserved feature of the Sema3E protein as it also existed in the medium from MDA-MB-468 human cancer cells expressing the *SEMA3E* gene (Fig. 2*B*). We got an indication of cross-reactivity with another human semaphorin when analysing the medium from MDA-MB-453 cells that are negative for SEMA3E transcripts (Fig. 2*B* compared with Fig. 1*A*). However, this other semaphorin was not detected in the medium from nontransfected 168FARN cells or mock-transfected COS-7 cells (Fig. 2*A*).

Next, we injected the Sema3E-transfected 168FARN cells into BALB/c mice and inspected the lungs for metastatic tumor growth after 20 to 31 days. When total lung weight was used as a measure of tumor growth, we found a highly significant growth of Sema3E transfected cells ($P = 0.0005$; Fig. 2*C*) but insignificant growth of parental ($P = 0.54$) and mock-transfected 168FARN cells ($P = 0.35$; Fig. 2*D*). Notably, massive tumor growth was observed exclusively in mice injected with Sema3E-transfected cells (Fig. 2*E*), resulting in increases in total lung weight of up to 400%. These *in vivo* experiments pointed to a potent activity of Sema3E as a promoter of metastatic growth in the lungs.

The expression of Sema3E in the metastatic lesions was detected by immunohistochemical staining of the mouse lungs using the anti-Sema3E antibodies. Sema3E-positive cells were seen invading the lung tissue at the interface between the tumors and lung tissue (Fig. 2*F*), and the staining could be blocked by Sema3E protein (Fig. 2*F*, *right corner inset*; see later for description of protein). Furthermore, the anti-mouse Sema3E antibody was able to detect human SEMA3E protein in solid tumors from breast cancer patients. In full agreement with the results of the reverse transcription-PCR (RT-PCR) analysis in Fig. 1 staining was not observed in tumors lacking SEMA3E mRNA (e.g., primary tumor 13 shown in Fig. 2*G*), whereas staining was seen in SEMA3E positive primary tumors and metastases (e.g., primary tumor 16 and metastasis 16, shown in Fig. 2*H* and *I*, respectively). In all cases, the specificity of the staining was confirmed by blocking with recombinant Sema3E protein (Fig. 2*F-I, insets*).

Sema3E stimulates endothelial cell migration and neurite outgrowth. Growth guidance factors are known to guide axonal growth by both attractive and repulsive means and semaphorins are known to act on both nerves and endothelial cells (11, 18). We hypothesized that the reason for the increased metastatic growth induced by Sema3E could be a growth attracting activity, which might be studied *in vitro* using endothelial cells or nerves. In particular, endothelial cell migration provides a possible link to metastasis through the process of angiogenesis (32). We first

examined the effect of Sema3E on the migration of SVEC4-10 lymph node endothelial cells (33). Conditioned medium from Sema3E transfected 168FARN and COS-7 cells stimulated SVEC4-10 cell migration 2- and 6-fold greater than conditioned medium from mock-transfected cells, respectively. Furthermore, following immunoprecipitation of Sema3E with anti-Sema3E antibodies the motility-stimulating activity in the medium was significantly decreased, showing that the stimulation was, at least partly, due to Sema3E (Fig. 3*A*). Next, we tested the effect of Sema3E on primary endothelial cell cultures from murine lung and liver (27). Lung microcapillary endothelial cells migrated in higher numbers in response to conditioned medium from 168FARN cells secreting Sema3E compared with conditioned medium from parental 168FARN cells, whereas HSE showed no signs of increased migration in response to conditioned medium containing Sema3E. In addition, as for SVEC4-10 cells the activity on lung microcapillary endothelial cells was shown to be Sema3E dependent using anti-Sema3E antibodies (Fig. 3*B*).

We also investigated the potential effect of Sema3E on neuronal cells through the use of the PC12-E2 pheochromocytoma cell line. We found that conditioned medium from COS-7 cells expressing Sema3E stimulated neurite growth in PC12-E2 cells to the same extent as NGF that is in agreement with findings previously reported by others using PC12 cells (ref. 34; Supplementary Fig. 1).

The activity of Sema3E on endothelial cell migration and neurite outgrowth supported our hypothesis that Sema3E is capable of promoting growth by attraction or direct stimulation.

Sema3E protein exists in different isoforms. As described above (Fig. 2*A* and *B*), the Sema3E protein exists in a number of different forms. To study the metastasis and growth promoting activities of Sema3E, we set out to characterize the Sema3E isoforms in detail. Related class 3 semaphorins are known to dimerize and undergo proteolytic processing by furin and furin-like convertases (24–26). The Sema3E protein contains the processing consensus sites, RXK/RR and RXXR (Fig. 4*A*), as well as a conserved COOH-terminal cysteine residue (Cys^{729}) situated where the disulfide bond is formed between monomers of other class 3 semaphorins (data not shown; refs. 24, 25). These structural features suggest that Sema3E like other class 3 semaphorins exists in monomeric, dimeric, and processed forms. The forms detectable with the Sema3E antibody would be full-size monomers (p87-Sema3E), full-size dimers (p87:p87-Sema3E), partially processed dimers (p87:p25-Sema3E), and released NH_2-terminal Sema3E (p61-Sema3E; Fig. 4*B*). The molecular size of these isoforms could explain the bands on the immunoblots in Fig. 2.

To test the accuracy of this interpretation, we generated constructs encoding myc-tagged wild-type, mutated, or truncated Sema3E proteins. In addition to a construct encoding full-length wild-type Sema3E [denoted Sema3E(+)(+)myc to indicate the presence of both the KRRFRR and RLPR sites], a second construct encoded Sema3E with the wild-type KRRFRR sequence but lacking the RLPR site [denoted Sema3E(+)(−)myc] and a third construct encoded Sema3E with the KRRFRR mutated into KRSFGG and lacking the RLPR site [denoted Sema3E(−)(−)myc]. Finally, a fourth construct encoded truncated Sema3E equal to p61-Sema3E without the KRRFRR site (i.e., p61-$Sema3E^{TR}$myc). These constructs were transfected into COS-7 cells, which allow efficient transient transfection and high expression after 24 hours. The resulting proteins were analyzed with the antibody to the NH_2 terminus of Sema3E as well as an antibody to the COOH-terminal myc-tag.

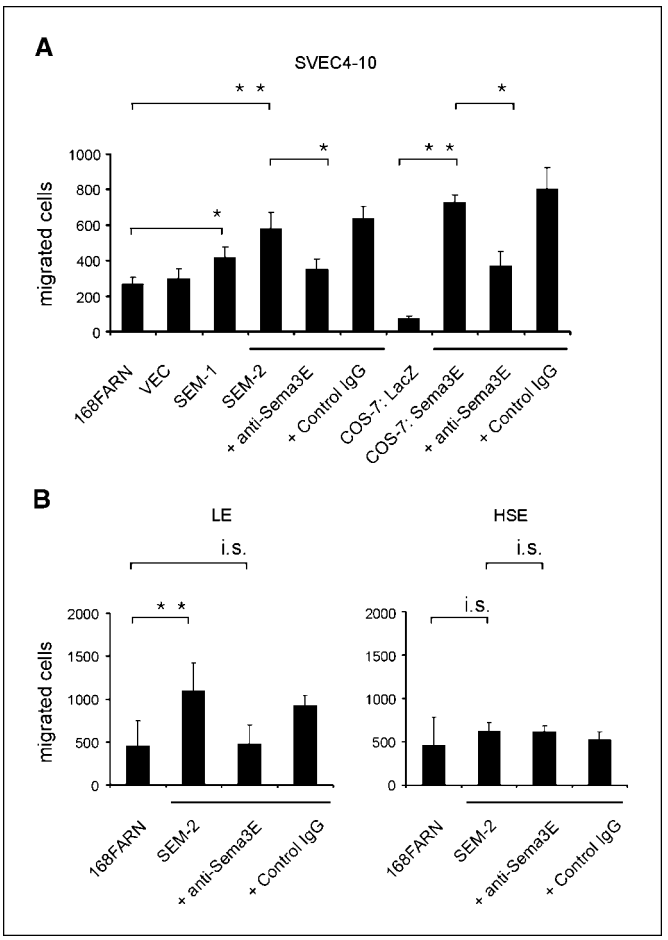

Figure 3. Sema3E stimulates endothelial cell migration. *A,* migration of SVEC4-10 endothelial cells in modified Boyden chambers. Cells were exposed to conditioned medium from parental 168FARN, mock-transfected (*VEC*), or Sema3E-transfected 168FARN cells (SEM-1 and SEM-2) as well as from COS-7 cells transiently transfected with plasmids encoding Sema3E or LacZ. In the case of conditioned medium from SEM-2 and COS-7:Sema3E, the SVEC4-10 cells were also exposed to medium that had been subjected to immunoprecipitation with rabbit polyclonal anti-Sema3E antibodies (+ anti-sema3E) or rabbit IgG (+ control IgG) before use. *B,* migration of lung microcapillary endothelial cells (*LE*) and HSE. Cells were exposed to conditioned medium from parental 168FARN cells and Sema3E-transfected 168FARN cells (clone SEM-2). In the case of conditioned medium from SEM-2, the cells were also exposed to medium that had been subjected to immunoprecipitation with Sema3E antibodies or rabbit IgG before use. *Columns,* means of three independent experiments done in triplicate; *bars,* SD. *, $P < 0.05$; **, $P < 0.02$; i.s., insignificant.

The Sema3E(+)(+)myc gave rise to a series of bands on an immunoblot stained with the Sema3E antibody. However, none of these bands were detected by an antibody to the myc tag indicating proteolytic release of the COOH-terminal sequence. In comparison, Sema3E(+)(−)myc produced proteins detectable with the myc antibody and the size of these bands corresponded to the expected p87:p87, p87:p25, and p25:p25 isoforms. However, the putative p61-Sema3E isoform was still spotted by the Sema3E antibody but not the myc antibody indicating that internal processing of Sema3E(+)(−) myc still occurred. This processing seemingly involved the KRRFRR site as it no longer took place in Sema3E(−)(−)myc proteins. These proteins almost entirely existed in the heaviest form, allegedly p87:p87, suggesting that proteolytic processing was completely abolished when both the RLPR and KRRFRR sites were compromised (Fig. 4*C*).

To study Sema3E dimerization, we then subjected the different proteins to treatment with a reducing agent. This led to the disappearance of the bands believed to represent the p87:p87 and p87:p25 isoforms thus supporting the composite nature of these forms. Notably, direct evidence for the p87:p87 isoform was found by examining the Sema3E(−)(−)myc protein. This protein existed solely in the ~87 kDa form after reduction, whereas it was only found in the ~174 kDa form before reduction as described above (Fig. 4*D*). Surprisingly, we also found evidence for the existence of p61:p61 dimers because expression of p61-Sema3E^{TR}myc produces a band of ~120 kDa, which is detectable with both the Sema3E and myc antibody, whereas this band disappears after reduction (Fig. 4*C* and *D*). However, it should be noted that this is likely to represent an artifact of overexpression because we lack evidence for the existence of this dimeric form in cells expressing endogenous Sema3E (as shown in Fig. 2).

Collectively, the analysis of Sema3E isoforms showed that Sema3E is expressed as full-length dimers and undergoes proteolytic conversion to a shorter form (i.e., p61-Sema3E).

p61-Sema3E isoform stimulates endothelial cell migration and neurite outgrowth. To answer the question of which isoform exerts the motility and growth promoting activity of Sema3E, we collected conditioned medium from COS-7 cells secreting wild-type Sema3E and separated the individual isoforms through combined heparin affinity purification and size exclusion chromatography. The resulting fractions were examined by immunoblot analysis and tested for activity towards SVEC4-10 cells. The immunoblot analysis revealed that p87:p87-Sema3E, p87-Sema3E, and p61-Sema3E were eluted in separate fractions following the purification procedure (Fig. 5*A*), and the functional assay showed that only the fractions containing p61-Sema3E (fractions 13 and 14) exerted any activity above background indicating that this

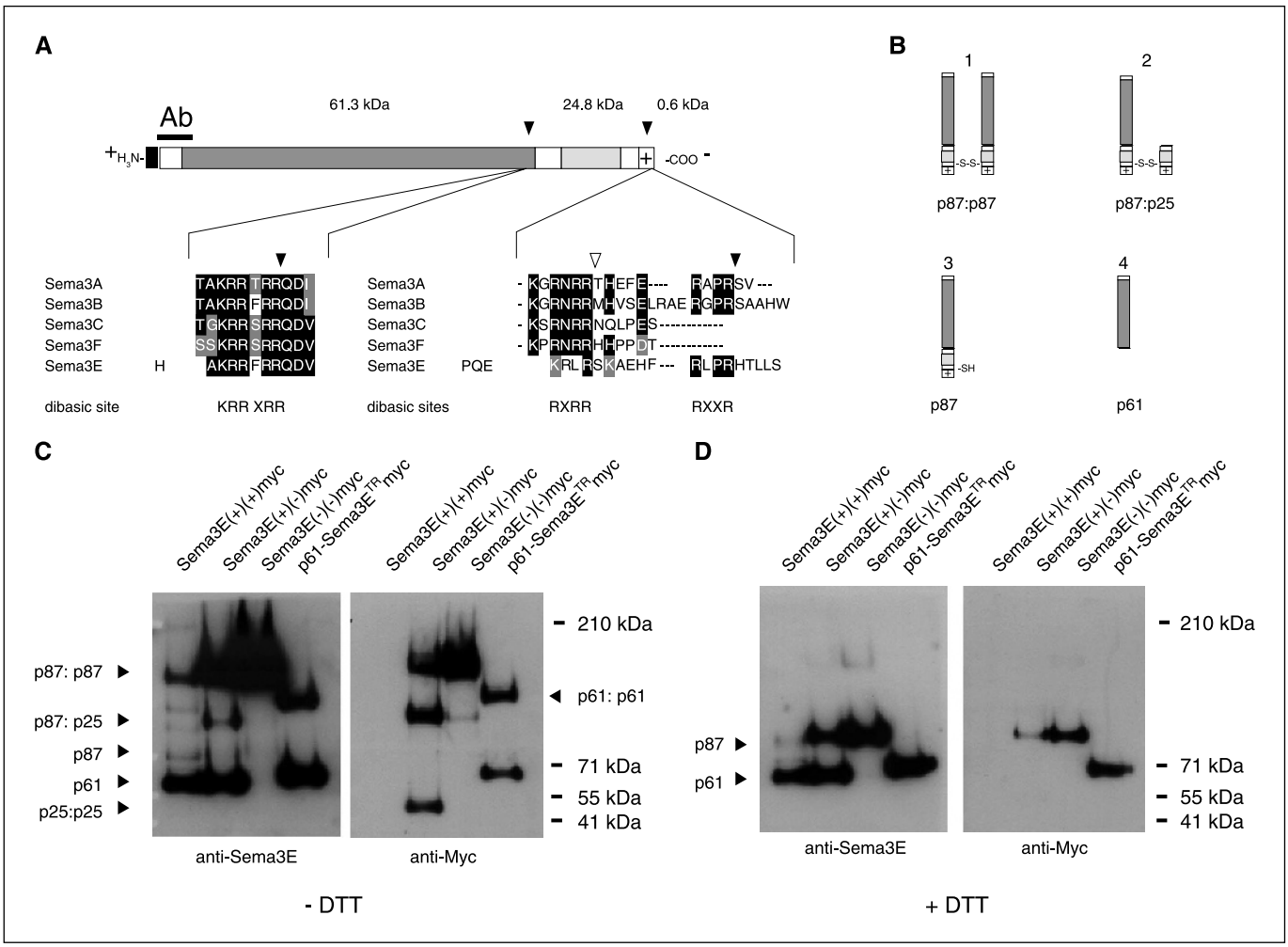

Figure 4. Sema3E protein undergoes dimerization and proteolytic processing. *A,* schematic representation of Sema3E showing the positions of the signal sequence (*black*), the SEMA domain (*dark gray*), the immunoglobulin-like domain (*light gray*), the basic COOH-terminal domain (+), and processing sites (*arrowheads*). The theoretical molecular weights of cleavage products are shown in kDa (*top*). The processing sites in Sema3E are aligned with other mouse class 3 semaphorins (*bottom*). Sema3E contains the consensus sites KRRXRR and RXXR (*black arrowheads*). Site present in other class 3 semaphorins but not in Sema3E (*open arrowhead*). Region to which polyclonal antiserum was produced (*Ab*). *B,* isoforms resulting from combined dimerization and proteolytic processing of Sema3E. Only the isoforms detectable with the antibody to Sema3E are shown. Constructs encoding Sema3E-myc were transfected into COS-7 cells, and after 24 hours, medium was collected and subjected to immunoblot analysis with antibodies to Sema3E and myc-tag (9B11), without reducing agent (*C*) or with the reducing agent DTT (*D*). In both (*C*) and (*D*) Sema3E(+)(+)myc denotes Sema3E with both the internal wild-type KRRFRR site and the RLPR site in the COOH terminus as opposed to Sema3E truncated in COOH terminus [Sema3E(+)(−)myc] and Sema3E with both a mutated internal site (KRRFRR->KRSFGG) and a truncated COOH terminus [Sema3E(−)(−)myc]. Proteins were separated using 3% to 8% TAE-polyacrylamide gels (Invitrogen). Within this range, the released COOH terminus is only detectable with the 9B11 antibody when no reducing agent is used.

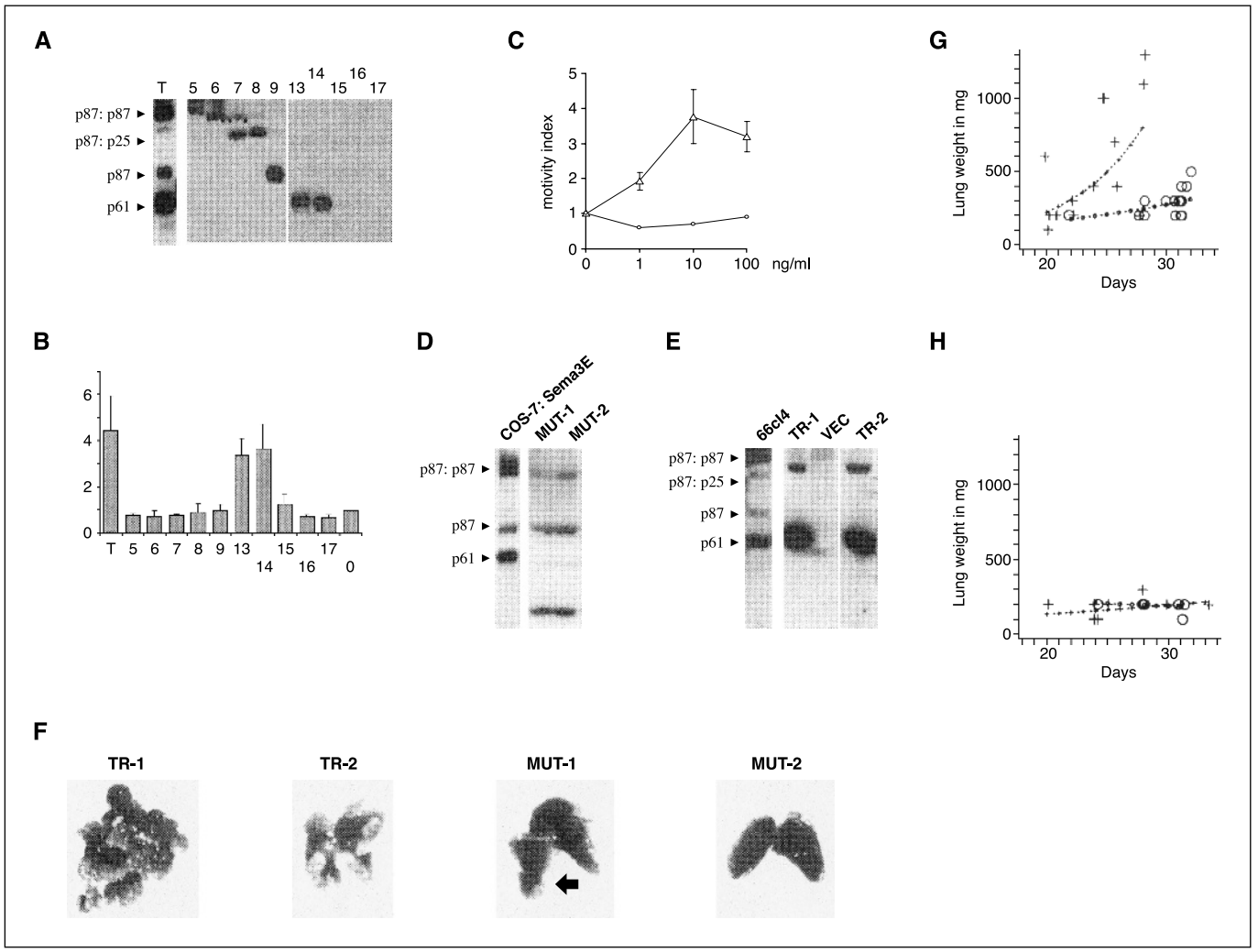

Figure 5. p61-Sema3E is both necessary and sufficient to promote endothelial cell migration and lung colonization. *A,* immunoblot analysis of Sema3E in total conditioned medium from COS-7 cells expressing Sema3E (*T*) and fractions of this medium after size exclusion chromatography (1,−9 and 13,−17). Fractions 10, 11, and 12 were omitted from analysis due to excessive amounts of BSA. *B,* total conditioned medium and fractions were investigated for activity in the SVEC4-10 migration assay. Activity was compared with conditioned medium from nontransfected COS-7 cells (0). *Columns,* averages of three independent experiments; *bars,* +SD. *C,* recombinant p61-Sema3E^{TR}myc was tested in the SVEC4-10 migration assay. Experiments were done thrice for p61-Sema3E^{TR}myc (△). *Bars,* ±SD. Only two experiments were done in the case of BSA (○). Immunoblot analysis of Sema3E expression in clonal populations of 168FARN cells transfected with (*D*) Sema3E(−)(+)myc (MUT-1 and MUT-2)or (*E*) construct encoding p61-Sema3E^{TR}myc (TR-1 and TR-2). Conditioned medium from either 66cl4 cells or COS-7 cells transfected with Sema3E constituted the controls for the positions of individual isoforms. *F,* examples of the macroscopic appearance of the lungs excised from mice injected with TR-1, TR-2, MUT-1, and MUT-2 cells. A few tumors were observed in the lungs from mice injected with MUT-1 cells (*arrow*). *G* and *H,* assessment of tumor growth by measurement of total lung weights at different time points following i.v. injection. Each point represents one mouse. *G,* mice injected with clone TR-1 (+, n = 14) and clone TR-2 (O, n = 14). *H,* mice injected with clone MUT-1 (+, n = 9) and clone MUT-2 (O, n = 9).

isoform was responsible for the increased migration of SVEC4-10 cells (Fig. 5*B*). To provide further evidence for the activity of p61-Sema3E, we then investigated the activity of purified, recombinant p61-Sema3E-myc proteins (p61-Sema3E^{TR}-mychis). Such proteins stimulated the motility of SVEC4-10 cells by up to 3.5-fold (Fig. 5*C*) and hence exerted an activity with a magnitude comparable with the activity present in fractionated conditioned medium containing p61-Sema3E. We therefore concluded that p61-Sema3E is required and sufficient for the motility-stimulating activity of Sema3E *in vitro*.

We also tested the fractionated conditioned medium on PC12-E2 cells. We found that both fractions containing p87:p87-Sema3E (fractions 5, 6, and 7) or p61-Sema3E (fractions 13 and 14) stimulated neurite outgrowth (Supplementary Fig. 2*A*). Then we investigated the activity of conditioned medium containing Sema3E(+)(+)myc, Sema3E(+)(−)myc, Sema3E(−)(−)myc, and p61-Sema3E^{TR}myc proteins as well as the effect of adding the furin inhibitor decanoyl-RVKR-chloromethylketone (26) to the assay. This way, we found that proteolysis is part of the mechanism underlying the growth stimulation by p87:p87-Sema3E and that the growth stimulation is probably due to p61-Sema3E formed as the result of this proteolysis (Supplementary Fig. 2*B*). The neurite outgrowth promoting activity of p61-Sema3E was subsequently confirmed by testing purified, recombinant p61-Sema3E^{TR}-mychis proteins (Supplementary Fig. 2*C*).

p61-Sema3E isoform stimulates experimental lung metastasis. Then we asked whether the processing of Sema3E into p61-Sema3E constituted the mechanism accounting for the experimental lung metastasis. To answer this question, we first transfected 168FARN cells with the construct encoding the

truncated Sema3E protein (p61-Sema3E^{TR}myc) or a construct encoding full-size Sema3E mutated in the internal KRRFRR site [Sema3E(−)(+)myc]. Clonal cell populations expressing this mutated semaphorin (clones MUT-1 and MUT-2) secreted p87 and p87:p87 isoforms, whereas both the p61 and the p87:p25 isoforms were absent (Fig. 5*D*). This confirmed that the alteration of the KRRFRR motif in Sema3E successfully abolishes the processing of that site. In comparison, 168FARN cells expressing p61-Sema3E^{TR}myc (clones TR-1 and TR-2) secreted a protein that migrated slightly above the wild-type p61 isoform as well as dimers of p61-Sema3E^{TR}-myc (Fig. 5*E*). We then injected the clonal populations in BALB/c mice. This resulted in visible and in some cases massive lung metastasis in those mice injected with p61-Sema3E^{TR}myc expressing cells whereas no metastasis (clone MUT-2) or only single lung tumors (clone MUT-1) resulted from injection of Sema3E(−)(+)myc expressing cells (Fig. 5*F*). Analysis of total lung weights revealed that mice injected with 168FARN cells expressing p61-Sema3E^{TR}myc showed an extremely significant increase in lung weights ($P < 0.0001$; Fig. 5*G*), which did not differ from the increase seen in mice, which received 168FARN cells expressing wild-type Sema3E in Fig. 2*C* ($P = 0.92$). Thus, cells expressing only p61-Sema3E^{TR}-myc were as metastatic as cells expressing all the isoforms of wild-type Sema3E. In comparison, mice injected with 168FARN cells expressing Sema3E(−)(+)myc showed no significant increase in lung weights ($P = 0.49$; Fig. 5*H*) and concomitantly differed from mice receiving 168FARN cells expressing wild-type Sema3E in Fig. 2*C* ($P = 0.041$). Thus, the inability to process p87:p87-Sema3E into p61-Sema3E renders the cells unable to grow in the lungs. Combined, the data presented in Figs. 2 and 5 showed that the p61-Sema3E isoform is not only sufficient but also necessary for the promotion of pulmonary cancer growth by Sema3E.

Clonal heterogeneity of cancer cell lines with respect to adhesion, protease expression, and chemotaxis may cause large variation in the metastatic behavior of individual subclones (35, 36). In the metastasis experiments presented in Figs. 2 and 5, clear signs of clonal variation were seen from the fact that clones expressing identical amounts of Sema3E behaved differently *in vivo*. Nevertheless, examples of massive lung metastasis were exclusively found in those groups of mice injected with 168FARN cells secreting p61-Sema3E alone or all isoforms including p61-Sema3E. Only these groups of mice showed increases in lung weight that rose exponentially and were significantly different from the other groups. Therefore, despite the clonal variation, there is a systematic effect of p61-Sema3E on lung metastasis.

Sema3E stimulates invasive growth and mitogen-activated protein kinase signaling. Finally, we sought to distinguish between two fundamentally different mechanisms as the cause of the increased metastatic potential of Sema3E-expressing 168FARN cells. One mechanism depicts autocrine stimulation by secreted Sema3E that would enable 168FARN cells to extravasate and grow invasively *in vivo*. In this case, we envisaged that 168FARN cells with an increased potential for metastatic growth would behave differently in an invasive growth assay *in vitro*. However, no difference was observed in the invasive growth of mock-transfected 168FARN cells, SEM-1, MUT-1, or TR-1 cells (Fig. 6*A*). Furthermore, conditioned medium containing the various forms of Sema3E protein had no effect on parental 168FARN cells in the same assay, although growth factors such as HGF did exert an effect (Fig. 6*B*; data not shown). The increased metastatic potential of Sema3E expressing cells may also result from increased proliferation of such cells or an increased adhesion of such cells to microvascular endothelial cells. However, neither 168FARN cell lines expressing Sema3E nor 168FARN cells treated with different isoforms of Sema3E adhered differently to endothelial cells compared with parental cells (Supplementary Fig. 3*A*). Moreover, 168FARN cells exhibited similar population doubling times irrespective of Sema3E expression or treatment (Supplementary Fig. 3*B*). When combined, these data indicate that the increased metastatic growth of Sema3E-expressing 168FARN cells is not attributed to an autocrine effect of Sema3E.

The alternative mechanism that could explain the increase in metastatic growth relies on the paracrine stimulation of endothelial cells by Sema3E secreted from the tumor cells in a manner contributing to angiogenesis. SVEC4-10 cells have been shown to mimic the process of angiogenesis when grown in extracts from basal membrane (29, 33). We placed pellets of SVEC4-10 cells inside gels formed from basal membrane extracts and observed the effect of growing the cells for 24 hours in the presence or absence of Sema3E isoforms. When grown in the presence of control conditioned medium containing alkaline phosphatase, invasive cells were observed sprouting from the pellet but keeping close cell-cell contacts. No difference was observed in this behavior when the medium contained p87:p87-Sema3E(−)(−)myc, whereas medium containing p61-Sema3E^{TR}-myc caused reproducible increases in the invasive growth response similar to the effect of HGF (Fig. 6*C*). Notably, no effect of p61-Sema3E^{TR}-myc was observed when testing the population doubling times of SVEC4-10 cells grown in the same kind of conditioned media (Supplementary Fig. 3*C*). Therefore, p61-Sema3E seems to act merely as a growth attractant for SVEC4-10 cells, and the observed increase in invasive growth may require that p61-Sema3E act synergistically with factors that stimulate proliferation.

To address the question of the signaling underlying the cellular response to p61-Sema3E, we investigated whether purified p61-Sema3E^{TR}-myc evokes changes in the activation status of extracellular signal–regulated kinase 1/2 (Erk1/2) in 168FARN or SVEC4-10 cells. The effect of adding p61-Sema3E^{TR}-myc to serum-starved 168FARN cells was not discernible from the effect of adding medium alone (Fig. 6*D*). However, in SVEC4-10 cells a marked effect was observed. The p61-Sema3E^{TR}-myc protein induced the activation of Erk1/2 beginning 5 minutes after addition. This was similar to the effect of HGF but different from medium that merely produced a short increase in Erk1/2 phosphorylation at 10 minutes (Fig. 6*E*). Thus, the activation of Erk1/2 correlated with the biological effect of p61-Sema3E^{TR}-myc in SVEC4-10 cells. The fact that similar treatments of 168FARN and SVEC4-10 cells only provoke a response in the latter is indicative of a paracrine mode of action.

Discussion

In our previous work, we found that the expression of Sema3E correlates with the ability to form lung metastasis in four murine adenocarcinoma cell models each consisting of paired metastatic and nonmetastatic cell lines from the same breast tumors (10). Here we have investigated the relevance of SEMA3E to human disease by examining human cancer cell lines and solid tumors from cancer patients. Furthermore, we have investigated the potential role of Sema3E in tumor progression

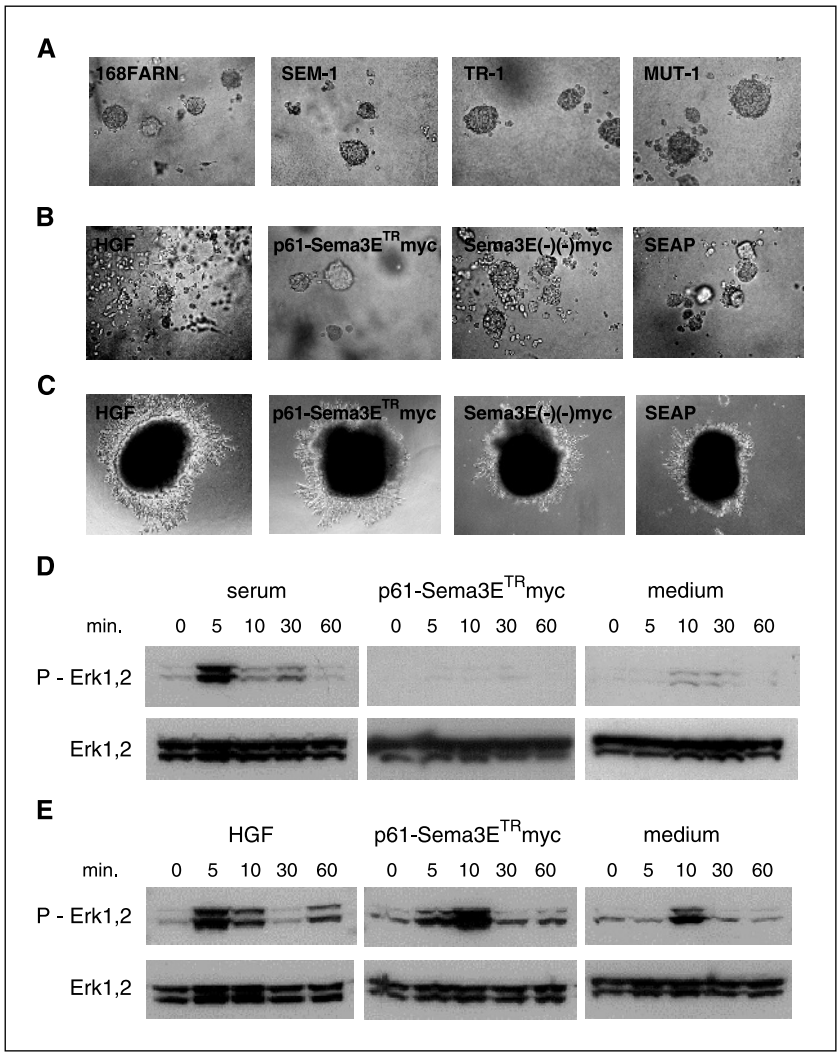

Figure 6. Sema3E stimulates MAPK activation and invasive growth in SVEC4-10 cells but not 168FARN tumor cells. *A* and *B,* invasive growth assay for 168FARN cells. The cells were cultured inside collagen I gels for 10 days. *A,* in one set of experiments, parental 168FARN cells and clonal derivatives (SEM-1, TR-1, and MUT-1) were tested in normal growth medium. *B,* in another set of experiments, parental 168FARN cells were grown in conditioned medium from HEK-293 cells plus HGF (20 ng/mL), or CM from the same cells 24 hours after transfection with constructs encoding p61-Sema3E^{TR}myc, Sema3E(−)(−)myc, or secreted alkaline phosphatase. Pictures in (*A*) and (*B*) represent the results from three experiments. *C,* invasive growth assay for SVEC4-10 cells. An aggregate of cells was placed inside a gel of extracellular matrix proteins and grown for 24 hours in the presence of conditioned medium from HEK-293 cells plus HGF (20 ng/mL), or conditioned medium from the same cells 24 hours after transfection with constructs encoding p61-Sema3E^{TR}myc, Sema3E(−)(−)myc, or secreted alkaline phosphatase. Pictures represent at least three experiments done in duplex. *D* and *E,* assessment of Erk1/2 activation in 168FARN and SVEC4-10 following serum starvation and exposure to either medium, medium plus 1% serum, or medium plus recombinant p61-Sema3E^{TR}myc (70 ng/mL) in the case of 168FARN cells (*D*) or medium, medium plus HGF (20 ng/mL), or medium plus p61-Sema3E^{TR}myc (70 ng/mL) in the case of SVEC4-10 cells (*E*). Immunoblots in (*D*) and (*E*) were analyzed with antibodies specific to Erk1/2 phosphorylated on Thr^{202}/Tyr^{204} (P-Erk1/2) as well as an antibody to Erk1/2 in general (Erk1/2) to verify similar loading.

and lung metastasis through the use of an experimental lung metastasis assay in combination with different functional assays *in vitro*.

Metastasis is a complex process involving several discrete steps that each places its own demands on the tumor cells for the expression of specific genes (3, 4). Therefore, cancer cells may express an array of metastasis associated genes and still remain nonmetastatic as long as they are deficient in any of the other steps needed to conclude the process (30, 31). In the present case, we found expression of SEMA3E in 69% of a limited number of solid tumors from breast cancer patients including regional metastases; but notably, not all regional metastases showed this expression. It may be speculated that SEMA3E is not needed for the metastasis of breast cancer cells to nearby lymph nodes but except for the fact that breast cancer metastasis to distant organs often proceeds via the lymphatic system, the presence or absence of SEMA3E expression in regional metastases, says little of the implication of SEMA3E in the later steps of the metastatic process. At the time of removal, a number of regional metastases may not contain cancer cells with the ability to metastasize further as shown in mouse tumor models (30). Furthermore, breast cancer is notorious for its propensity to metastasize to bones (2); therefore, it is possible that Sema3E, if associated stringently with lung metastasis, would not be detected in a major part of metastatic breast cancers. To resolve this issue, a more detailed analysis is needed including more samples and clinical data on individual patients.

With respect to cancer cell lines, we found SEMA3E transcripts in cell lines such as MDA-MB-231 and MDA-MB-468, which are known to metastasize to the lungs in nude mice (37), whereas we did not detect transcripts in the nonmetastatic cancer cell line, MDA-MB-453 or human mammary epithelial cells. This is consistent with a role of SEMA3E in lung metastasis and in accordance with our previous findings of Sema3E transcripts in all murine cell lines that produce experimental lung metastasis (10). However, we also found transcripts in human cancer cell lines, such as MCF-7 and BT-20, known to have low metastatic potential in nude mice (37). This indicates that SEMA3E is not sufficient to induce lung metastasis of human cancer cells, but because MCF-7 and BT-20 cells may be deficient in several steps of the metastatic process, the presence of SEMA3E transcripts in these cell lines does not exclude the proposed role of SEMA3E in lung metastasis. In general, caution should be exerted when considering the low metastatic potential of human cancer cell lines in rodents. Other reports suggest that the growth of human cancer cells is still hampered by the immune system in nude mice (38, 39), whereas in severe combined immunodeficient mice (SCID mice) some cancer

cell lines will metastasize only to engrafted human tissue but not homologous murine tissue pointing to the existence of species-specific mechanisms or incompatible tumor-host interactions that negatively affects the metastatic growth of human cancer cells in rodents (40). For these reasons, it is difficult to say whether SEMA3E expression correlates with lung metastasis in human cancer cell lines, and for the same reasons, we chose not to use any of the existing human breast cancer cell models for the further studies of Sema3E.

The complexity of the metastatic process makes it essential to exploit experimental tumor models that are carefully characterized and allow the study of specific genes during individual steps of the metastatic cascade. In the present case, we have used the nonmetastatic cell line, 168FARN, which is derived from a murine mammary adenocarcinoma (30, 31). Experiments exploiting the neomycin resistance of these cells to track their dissemination *in vivo* have shown that 168FARN cells can be found in the lungs 24 hours after i.v. injection, but they rarely grow into tumors (10, 31). This indicates that 168FARN cells, although capable of extravasation, are incapable of metastatic growth within the lung parenchyma. In our previous work, the correlation between Sema3E expression and metastatic potential was particularly strong when using the experimental lung metastasis assay, indicating that Sema3E is causally involved in the final steps of metastasis to the lungs (10). Due to the ability of 168FARN cells to extravasate combined with the inability to grow in the lungs, 168FARN cells are ideally suited for use in the investigation of Sema3E activity during the concluding steps of the metastatic cascade. The results of this work are presented here and provide evidence for the suggested role of Sema3E in lung colonization.

The "seed and soil" hypothesis proposed by Stephen Paget in 1889 states that metastasis form only when the cancer cells (the "seeds") and the specific organ environments (the "soils") are compatible (2). Today, this hypothesis is supported by both clinical and experimental data, and it is generally accepted that metastatic growth and primary tumor growth may rely on different, tissue-specific mechanisms (3, 4). Interestingly, Sema3E seems to fit the description of a property of the "seeds" that influences the "soil" (in this case the lungs) to facilitate the formation of metastasis. First, Sema3E stimulates the metastatic growth of 168FARN cells, which in the absence of Sema3E are merely seeded in the lungs but grow poorly (10, 30, 31). Second, Sema3E stimulates the motility of lung microcapillary endothelial cells suggesting that Sema3E mediates tumor-endothelial cell interaction and may facilitate lung metastasis by contributing to a local angiogenic response. Curiously, besides attracting lung endothelial cells, Sema3E attracts lymph node endothelial cells but has no effect on the migration of liver endothelial cells. Moreover, Sema3E seems dispensable for 168FARN tumors growing in the mammary fat pad or subcutis (10, 30, 31). These observations suggest that the effect of Sema3E may be limited to certain organs and tissues, perhaps reflecting organ-specific properties of the endothelial cells or the extracellular microenvironments. The classic view on angiogenesis depicts a balance between ubiquitously existing angiogenic factors and antiangiogenic factors, which may be shifted before tumor angiogenesis in a process termed the angiogenic switch (32). However, the existence of tissue-specific factors with angiogenic activity (41) and the differential influence of different organ sites on the expression of angiogenic molecules in cancer cells (42), point to the existence of organ-specific regulation of angiogenesis. This phenomenon may be essential for our understanding of the organ-specific metastasis of cancers with implications for future therapy (1). Meanwhile, our data presents Sema3E as a novel candidate for taking part in lung metastasis and specific tumor-endothelial cell interaction, and we propose that these data are best understood and further developed in the context of the "seed and soil" hypothesis and the theory of organ-specific regulation of angiogenesis.

The expression profiles of class 3 semaphorins in cancer have for some time indicated that individual class 3 semaphorins might have opposite roles during tumor progression (10, 20); but up until this moment, functional studies have only ascertained the roles of class 3 semaphorins (i.e. SEMA3B and SEMA3F) as important tumor suppressors (21–23) and SEMA3F and SEMA3A as negative regulators of angiogenesis (18, 19, 23). In the present study showing metastasis-promoting activity of a class 3 semaphorin, evidence is provided for the functional dichotomy of class 3 semaphorins in tumor progression. This dichotomy is striking as Sema3E and the tumor-suppressive semaphorins have analogous and partially overlapping expression profiles and activities during embryonic development of the nervous system (43). Studies of *Sema3A* and *neuropilin-1* knockout mice (44, 45) and receptor ligand studies *in vitro* (46) also point to extensive redundancy in semaphorin signaling pathways raising the question of how structurally similar semaphorins acquire the necessary distinction between them, which allows for the opposite biological functions during tumor progression. It is interesting that the metastasis promoting function of Sema3E is associated with a short form lacking COOH-terminal domains. Meanwhile, all available data indicate that the tumor suppressive and growth repelling activities of class 3 semaphorins are associated with the neuropilin-binding capacity of full-length, dimeric forms of these semaphorins (18, 19, 23, 45). It is furthermore intriguing that the short form of Sema3E stems from furin-dependent proteolytic processing; meanwhile, this sort of processing has been shown to down-regulate the repellent activity of class 3 semaphorins in neurobiology. All class 3 semaphorins share the dibasic motifs, which are present in Sema3E, and they are equally prone to proteolytic conversion (26). Thus, it seems that furin has the capacity to cause distinctions between the structures of class 3 semaphorin ligands, which may be of functional importance.

During tumor progression furin and related proprotein convertases are frequently expressed in tumor cell lines and human cancers including those of the breast (47), head and neck (48), and lung (49). In particular, the expression of furin correlates with aggressiveness and metastasis in human head and neck cancer (48), and whereas the *furin* gene is not expressed in normal lung tissue, it is highly expressed in certain lung tumors (49). These data support the specific relevance of furin expression in lung metastasis and tumor growth within the lung parenchyma. We propose that furin and related proprotein convertases may add to an increased malignancy by converting semaphorins into isoforms with growth-promoting capabilities, as shown here for Sema3E. Moreover, by severing the full-length dimeric forms of semaphorins, it is also possible that furin contributes to the down-regulation of the tumor-suppressive activities of SEMA3B and SEMA3F. Thus, future research may benefit from the investigation of how semaphorin activities are regulated by furin expression during tumor progression.

In addendum, it was recently shown that unlike other class 3 semaphorins, Sema3E binds PlexinD1 independently of neuropilins. Moreover, PlexinD1 is expressed in endothelial cells and seems to mediate cell repulsion in response to Sema3E stimulation (50). We have found that p61-Sema3E is capable of binding PlexinD1 expressed on the surface of COS-7 cells, and that PlexinD1 is expressed in both 168FARN tumor cells and SVEC4-10 endothelial cells (data not shown). However, considering the fact that Sema3E only seems to affect SVEC4-10 but not 168FARN cells, it seems unlikely that the PlexinD1 receptor alone is mediating the activity of p61-Sema3E described here. In addition, we have observed an activity opposite to the repelling activity described by Gu et al. Therefore, it may be speculated that p61-Sema3E mediates its effect via a complex of PlexinD1 and other associated molecules, which are able to convert the outcome of plexin signaling from repulsion to attraction. Further studies are in progress to answer this question *in vitro* and *in vivo*.

Acknowledgments

Received 12/2/2004; revised 4/13/2005; accepted 5/4/2005.

Grant support: Danish Cancer Society and Italian Association for Cancer Research.

The costs of publication of this article were defrayed in part by the payment of page charges. This article must therefore be hereby marked *advertisement* in accordance with 18 U.S.C. Section 1734 solely to indicate this fact.

We thank Dr. Alain Chedotal for providing the construct encoding Sema3E(+)(−)myc and Dr. Jun-Ichi Hamada for providing the HSE and lung microcapillary endothelial cells.

References

1. Fidler IJ. Critical determinants of cancer metastasis: rationale for therapy. Cancer Chemother Pharmacol 1999;43:S3–10.
2. Paget S. The distribution of secondary growths in cancer of the breast (republication of Lancet 1889;1: 571–3). Cancer Metastasis Rev 1989;8:98–101.
3. Fidler IJ. The pathogenesis of cancer metastasis: the 'seed and soil' hypothesis revisited. Nat Rev Cancer 2002; 3:453–8.
4. Chambers AF, Groom AC, MacDonald IC. Dissemination and growth of cancer cells in metastatic sites. Nat Rev Cancer 2002;2:563–72.
5. Liotta LA, Kohn EC. The microenvironment of the tumour-host interface. Nature 2001:411:375–9.
6. Taichman RS, Cooper C, Keller ET, Pienta KJ, Taichman NS, McCauley LK. Use of the stromal cell-derived factor-1/CXCR4 pathway in prostate cancer metastasis to bone. Cancer Res 2002;62:1832–7.
7. Yin JJ, Mohammad KS, Kakonen SM, et al. A causal role for endothelin-1 in the pathogenesis of osteoblastic bone metastases. Proc Natl Acad Sci U S A 2003;100: 10954–9.
8. Kang Y, Siegel PM, Shu W, et al. Multigenic program mediating breast cancer metastasis to bone. Cancer Cell 2003;3:537–49.
9. Semaphorin Nomenclature Committee. Unified nomenclature for the semaphorins/collapsins. Cell 1999;97:551–2.
10. Christensen CRL, Klingelhoefer J, Tarabykina S, Hulgaard EF, Kramerov D, Lukanidin E. Transcription of a novel mouse semaphorin gene, M-semaH, correlates with the metastatic ability of mouse tumor cell lines. Cancer Res 1998;58:1238–44.
11. Tessier-Lavigne M, Goodman CS. The molecular biology of axon guidance. Science 1996;274:1123–33.
12. Gitler AD, Lu MM, Epstein JA. PlexinD1 and semaphorin signaling are required in endothelial cells for cardiovascular development. Dev Cell 2004;7:107–16.
13. Serini G, Valdembri D, Zanivan S, et al. Class 3 semaphorins control vascular morphogenesis by inhibiting integrin function. Nature 2003;424:391–7.
14. Park KW, Crouse D, Lee M, et al. The axonal attractant Netrin-1 is an angiogenic factor. Proc Natl Acad Sci U S A 2004;101:16210–5.
15. Wang B, Xiao Y, Ding BB, et al. Induction of tumor angiogenesis by Slit-Robo signaling and inhibition of cancer growth by blocking Robo activity. Cancer Cell 2003:4:19–29.
16. Basile JR, Barac A, Zhu T, Guan KL, Gutkind JS. Class IV semaphorins promote angiogenesis by stimulating Rho-initiated pathways through plexin-B. Cancer Res 2004;64:5212–24.
17. Giordano S, Corso S, Conrotto P, et al. The semaphorin 4D receptor controls invasive growth by coupling with Met. Nat Cell Biol 2002;4:720–4.
18. Miao HQ, Soker S, Feiner L, Alonso JL, Raper JA, Klagsbrun M. Neuropilin-1 mediates collapsin-1/Semaphorin III inhibition of endothelial cell motility: functional competition of collapsin-1 and vascular endothelial growth factor-165. J Cell Biol 1999;146:233–42.
19. Kessler O, Shraga-Heled N, Lange T, et al. Semaphorin-3F is an inhibitor of tumor angiogenesis. Cancer Res 2004;64:1008–15.
20. Sekido Y, Bader S, Latif F, et al. Human semaphorins A(V) and IV reside in the 3p21.3 small cell lung cancer deletion region and demonstrate distinct expression patterns. Proc Natl Acad Sci U S A 1996;93:4120–5.
21. Tomizawa Y, Sekido Y, Kondo M, et al. Inhibition of lung cancer cell growth and induction of apoptosis after reexpression of 3p21.3 candidate tumor suppressor gene SEMA3B. Proc Natl Acad Sci USA 2001;98:13954–9.
22. Xiang R, Davalos AR, Hensel CH, Zhou XJ, Tse C, Naylor SL. Semaphorin 3F gene from human 3p21.3 suppresses tumor formation in nude mice. Cancer Res 2002;62:2637–43.
23. Bielenberg DR, Hida Y, Shimizu A, et al. Semaphorin 3F, a chemorepulsant for endothelial cells, induces a poorly vascularized, encapsulated, nonmetastatic tumor phenotype. J Clin Invest 2004;114:1260–71.
24. Klosterman A, Lohrum M, Adams RH, Puschel AW. The chemorepulsive activity of the axonal guidance signal semaphorin D requires dimerization. J Biol Chem 1998;273:7326–31.
25. Koppel AM, Raper JA. Collapsin-1 covalently dimerizes, and dimerization is necessary for collapsing activity. J Biol Chem 1998;273:15708–13.
26. Adams RH, Lohrum M, Klosterman A, Betz H, Pueschel AW. The chemorepulsive activity of secreted semaphorins is regulated by Furin-dependent proteolytic processing. EMBO J 1997;16:6077–86.
27. Hamada J, Cavanaugh PG, Lotan O, Nicolson GL. Separable growth and migration factors for large-cell lymphoma cells secreted by microvascular endothelial cells derived from target organs for metastasis. Br J Cancer 1992;66:349–54.
28. Barberis D, Artigiani S, Casazza A. Plexin signaling hampers integrin-based adhesion, leading to Rho-kinase independent cell rounding, and inhibiting lamellipodia extension and cell motility. FASEB J 2004;18:592–4.
29. Ambartsumian N, Christensen C, Lukanidin E. Endothelial cell invasion assay. In: Celis J, editor. Cell biology: a laboratory handbook, third ed. San Diego: Academic Press; 2005. In press.
30. Aslakson CJ, Miller FR. Selective events in the metastatic process defined by analysis of the sequential dissemination of subpopulations of a mouse mammary tumor. Cancer Res 1992;52:1399–405.
31. Aslakson CJ, Rak JW, Miller BE, Miller FR. Differential influence of organ site on three subpopulations of a single mouse mammary tumor at two distinct steps in metastasis. Int J Cancer 1992;47:466–72.
32. Hanahan D, Folkman J. Patterns and emerging mechanisms of the angiogenic switch during tumorigenesis. Cell 1996;86:353–64.
33. O'Connell KA, Edidin M. A mouse lymphoid endothelial cell line immortalized by simian virus 40 binds lymphocytes and retains functional characteristics of normal endothelial cells. J Immunol 1990;144:521–5.
34. Sakai T, Furuyama T, Ohoka Y, et al. Mouse semaphorin H induces PC12 cell neurite outgrowth activating Ras-mitogen-activated protein kinase signaling pathway via Ca(2+) influx. J Biol Chem 1999;274: 29666–71.
35. Taniguchi S, Iwamura T, Kitamura N, Yamanari H, Setoguchi T. Heterogeneities of attachment, chemotaxis, and protease production among clones with different metastatic potentials from a human pancreatic cancer cell line. Clin Exp Metastasis 1994;12:238–44.
36. Hill RP, Young SD, Cillo C, and Ling V. Metastatic cell phenotypes: quantitative studies using the experimental metastasis assay. Cancer Rev 1986;5:118–51.
37. Lacroix M, Leclercq G. Relevance of breast cancer cell lines as models for breast tumours: an update. Breast Cancer Res Treat 2004;83:249–89.
38. Price JE. Metastasis from human breast cancer cell lines. Breast Cancer Res Treat 1996;39:93–102.
39. Phillips RA, Jewett MAS, Gallie BL. Growth of human tumors in immune-deficient SCID mice and nude mice. Curr Top Microbiol Immunol 1989;152:259–63.
40. Shtivelman E, Namikawa R. Species-specific metastasis of human tumor cells in the severe combined immunodeficiency mouse engrafted with human tissue. Proc Natl Acad Sci U S A 1995;92:4661–5.
41. LeCouter J, Lin R, Ferrara N. Endocrine gland-derived VEGF and the emerging hypothesis of organ-specific regulation of angiogenesis. Nat Med 2002;8:913–7.
42. Gutman M, Singh RK, Xie K, Bucana CD, Fidler IJ. Regulation of IL-8 expression in human melanoma cells by the organ environment. Cancer Res 1995;55: 2470–5.
43. Pozas E, Pascual M, Nguyen Ba-Charvet KT, et al. Age-dependent effects of secreted semaphorins 3A, 3F, and 3E on developing hippocampal axons: *in vitro* effects and phenotype of semaphorin 3A (−/−) mice. Mol Cell Neurosci 2001;18:26–43.
44. Behar O, Golden JA, Mashimo H, Schoen FJ, Fishman MC. Semaphorin III is needed for normal patterning and growth of nerves, bones and heart. Nature 1996;383:525–8.
45. Gu C, Rodriguez ER, Reimert DV, et al. Neuropilin-1 conveys semaphorin and VEGF signaling during neural and cardiovascular development. Dev Cell 2003;5:45–57.
46. Tamagnone L, Comoglio PM. Signalling by semaphorin receptors: cell guidance and beyond. Trends Cell Biol 2000;10:377–83.
47. Cheng M, Watson PH, Paterson JA, Seidah N, Chretien M, Shiu RP. Pro-protein convertase gene expression in human breast cancer. Int J Cancer 1997; 71:966–71.
48. Bassi DE, Lopez De Cicco R, Mahloogi H, Zucker S, Thomas G, Klein-Szanto AJ. Furin inhibition results in absent or decreased invasiveness and tumorigenicity of human cancer cells. Proc Natl Acad Sci U S A 2001;98: 10326–31.
49. Mbikay M, Sirois F, Yao J, Seidah NG, Chretien M. Comparative analysis of expression of the proprotein convertases furin, PACE4, PC1 and PC2 in human lung tumours. Br J Cancer 1997;75:1509–14.
50. Gu C, Yoshida Y, Livet J, Reimert DV, Mann F, Merte J. Semaphorin 3E and plexin-D1 control vascular pattern independently of neuropilins. Science 2005;307:265–8.

Proteolytic Processing Converts the Repelling Signal Sema3E into an Inducer of Invasive Growth and Lung Metastasis

Claus Christensen, Noona Ambartsumian, Giorgio Gilestro, et al.

Cancer Res 2005;65:6167-6177.